An Evaluation of a Hybrid, Terrain-Following Vertical Coordinate in the WRF-Based RAP and HRRR Models

JEFFREY BECK

Cooperative Institute for Research in the Atmosphere, Colorado State University, and NOAA/OAR/ESRL/Global Systems Laboratory, Boulder, Colorado

JOHN BROWN

NOAA/OAR/ESRL/Global Systems Laboratory, Boulder, Colorado

JIMY DUDHIA, DAVID GILL, TRACY HERTNEKY, JOSEPH KLEMP, WEI WANG, AND CHRISTOPHER WILLIAMS

National Center for Atmospheric Research, Boulder, Colorado

MING HU, ERIC JAMES, JAYMES KENYON, AND TANYA SMIRNOVA

Cooperative Institute for Research in Environmental Sciences, University of Colorado Boulder, and NOAA/OAR/ESRL/Global Systems Laboratory, Boulder, Colorado

JUNG-HOON KIM

School of Earth and Environmental Sciences, Seoul National University, Seoul, South Korea

(Manuscript received 23 July 2019, in final form 30 March 2020)

ABSTRACT

A new hybrid, sigma-pressure vertical coordinate was recently added to the Weather Research and Forecasting (WRF) Model in an effort to reduce numerical noise in the model equations near complex terrain. Testing of this hybrid, terrain-following coordinate was undertaken in the WRF-based Rapid Refresh (RAP) and High-Resolution Rapid Refresh (HRRR) models to assess impacts on retrospective and real-time simulations. Initial cold-start simulations indicated that the majority of differences between the hybrid and traditional sigma coordinate were confined to regions downstream of mountainous terrain and focused in the upper levels. Week-long retrospective simulations generally resulted in small improvements for the RAP, and a neutral impact in the HRRR when the hybrid coordinate was used. However, one possibility is that the inclusion of data assimilation in the experiments may have minimized differences between the vertical coordinates. Finally, analysis of turbulence forecasts with the new hybrid coordinate indicate a significant reduction in spurious vertical motion over the full length of the Rocky Mountains. Overall, the results indicate a potential to improve forecast metrics through implementation of the hybrid coordinate, particularly at upper levels, and downstream of complex terrain.

1. Introduction

The traditional sigma, terrain-following coordinate (e.g., Phillips 1957; Gal-Chen and Somerville 1975) has been employed successfully in numerical weather prediction (NWP) for many years. While it defines the terrain as the lower boundary condition of the model, avoiding certain pitfalls of other vertical coordinate systems, the sigma, terrain-following coordinate is known to have some drawbacks. For example, numerical truncation errors can occur over areas of steep terrain, where coordinate surfaces depart significantly from a horizontal orientation. These errors are produced during the calculation of the horizontal pressure gradient force and have been well documented in the literature (e.g., Kurihara 1968; Mahrer 1984;

Corresponding author: Jeffrey Beck, jeff.beck@noaa.gov

DOI: 10.1175/WAF-D-19-0146.1

Mesinger and Janjić 1985). As a result, spurious horizontal and vertical accelerations/decelerations are introduced into the model equations, often resulting in vertical columns of numerical noise in the model wind field (and ultimately other variables) over mountainous regions.

Given the impact these errors can have on model variable accuracy and resulting forecasts (e.g., Park et al. 2016), a number of modifications to the sigma, terrain-following vertical coordinate have been developed to mitigate these problems (e.g., Schär et al. 2002; Zängl 2003; Klemp 2011). One such effort, outlined in Klemp (2011), involves gradually transitioning the terrain-following sigma coordinate to a height-based coordinate at a specified vertical level, reducing artificial noise associated with the traditional sigma coordinate. A number of National Center for Atmospheric Research (NCAR) models have employed a pressure-based version of this hybrid vertical coordinate, including the Community Atmosphere Model (CAM; Neale et al. 2012) and initial versions of the Model for Prediction Across Scales [MPAS; see appendix of Park et al. (2013)]. Continuing along these lines, NCAR recently completed work to add a pressure-based, hybrid vertical coordinate option to the Weather Research and Forecasting (WRF) Model, where vertical coordinate surfaces gradually transition from sigma to isobaric levels. Initial tests showed promising results for idealized cases with a considerable reduction in small-scale, spurious wind field disturbances. Based on these preliminary findings, further research was undertaken within the Global Systems Division (GSD) of NOAA/ESRL and the Developmental Testbed Center (DTC) to evaluate this new hybrid coordinate within the WRF-based, hourly updated, 13-km Rapid Refresh (RAP) and 3-km High-Resolution Rapid Refresh (HRRR) regional models (Smith et al. 2008; Benjamin et al. 2016). A brief description of the new hybrid coordinate will be presented in section 2, followed by analyses of RAP and HRRR simulations in sections 3 and 4. Finally, select HRRR case study simulations will be highlighted in section 5, with a summary of the principal findings presented in section 6.

2. The hybrid, sigma-pressure, terrain-following coordinate

As with the implementation of the hybrid vertical coordinate in the hydrostatic version of MPAS (Park et al. 2013), the vertical coordinate η in the latest releases of the WRF-ARW model is defined based on p_d, or the dry hydrostatic pressure:

$$p_d = B(\eta)(p_s - p_t) + [\eta - B(\eta)](p_0 - p_t) + p_t, \quad (1)$$

where p_s is the hydrostatic surface pressure, p_t is the model top pressure, and p_0 is the reference sea level pressure. The term $B(\eta)$ is a function that describes the relative weights given to the sigma and pure pressure components of the hybrid vertical coordinate [Eq. (3) in Park et al. (2019)]. To gradually transition from sigma to pressure coordinate surfaces, $B(\eta)$ follows a cubic polynomial, constrained by a user-defined parameter η_c, used to describe the shape of the third-order polynomial and to determine the level above which all vertical coordinate surfaces will be purely isobaric. Much more detail on these equations and the relation of the hybrid coordinate to the pure hydrostatic pressure can be found in Park et al. (2019) and Skamarock et al. (2019), while Skamarock et al. (2008) provides a description of the original sigma, terrain-following coordinate.

3. Idealized simulations

Prior to full-scale testing with real atmospheric initial conditions, it is beneficial to evaluate implementation of the new vertical coordinate through simplified, idealized experiments. Therefore, two-dimensional advection simulations were conducted to isolate terrain-induced differences between the sigma, terrain-following and hybrid coordinates. In addition to vertical velocity, perturbation values of potential temperature and the U component of the wind were plotted to compare coordinate systems and to evaluate reductions to artificial accelerations/decelerations when using the hybrid coordinate.

a. Experiment design

Simulations followed the method outlined in Schär et al. (2002) for both the sigma, terrain-following and hybrid coordinates. Figure 1 shows the position of the vertical coordinate surfaces for 1) the sigma, terrain-following coordinate and 2) the hybrid coordinate for the simulations, where the maximum idealized obstacle height was set at 2000 m, the depth of the atmosphere was 20 km above the nonelevated terrain, and the fixed vertical grid spacing between coordinate surfaces was set to 500 m. A simplified shear profile was used, containing a stagnant atmosphere below 6 km (above the nonelevated terrain), but above which, the U component of the wind gradually increased to 20 m s^{-1} at 10 km above the nonelevated terrain, and remained at that speed up to the model top. Both simulations used a 1-km horizontal grid spacing. Finally, the transition sigma level η_c for the hybrid coordinate, above which the vertical coordinate transitions to purely isobaric levels, was set to 0.3.

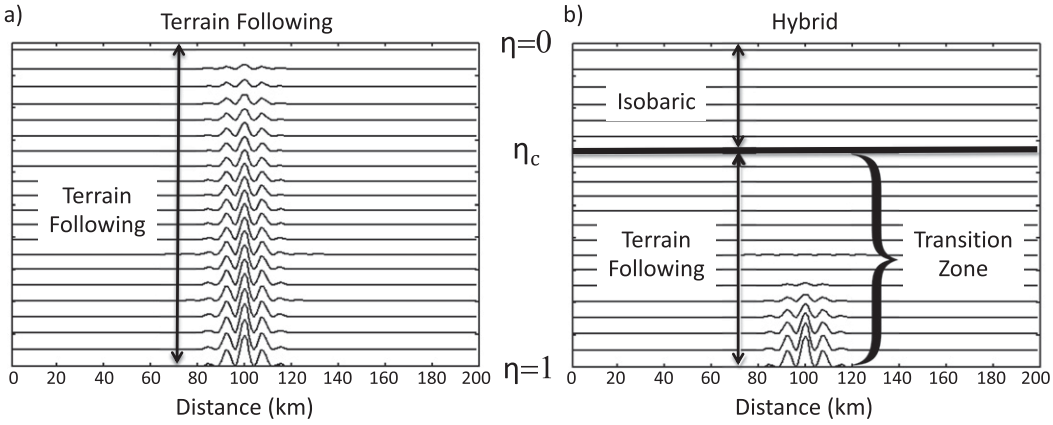

FIG. 1. Two-dimensional plots of idealized coordinate surfaces η for the (a) sigma, terrain-following and (b) hybrid coordinates. The vertical level η_c represents the user-defined point above which the hybrid coordinate transitions to purely isobaric vertical levels.

b. Results

Within the purely terrain-following coordinate, reflections from the idealized mountain range are apparent in the vertical coordinate surfaces up to the model top (Fig. 1a), while vertical levels within the hybrid coordinate simulation are slowly transitioned to isobaric levels, resulting in nearly flat coordinate surfaces well below the transition level (Fig. 1b). In addition, it is evident from the idealized advection results (Figs. 2a–f) that the hybrid coordinate is able to significantly dampen the artificial noise generated downwind of the idealized mountain range in the center of the domain. Upper-level vertical velocity (Figs. 2a,b), the U component of the wind (Figs. 2c,d), and upper-level potential temperature (Figs. 2e,f) all show improvements in the propagation of artificial noise when using the hybrid vertical coordinate. In addition, any spurious waves that were generated downwind when using the hybrid coordinate result in variable perturbations of the same magnitude as those found upwind of the idealized mountain range.

The overall goal of the hybrid vertical coordinate was to allow for as much of the model domain to be defined by an isobaric coordinate as possible, yet at the same time avoiding sharp gradients or discontinuities in the thickness of vertical coordinate surfaces. This requirement is particularly important over complex terrain, where the intention is to minimize numerical artifacts such as spurious reflections of vertically propagating waves. Further, the user-defined variable η_c is critical to achieving a balance between avoiding numerical problems with the purely sigma coordinate and introducing new problems (e.g., a large vertical Courant number) by making the coordinate layers excessively thin over the highest terrain. In the previously described idealized simulations, a value of η_c equal to 0.2–0.3 was found to provide for an ideal transition to isobaric coordinates in the upper 2/3–1/4 of the model domain. However, this value is also dependent on the regional domain chosen for the model. For domains containing large variations in terrain elevation, further testing of different η_c values may be required to obtain an optimal transition value, minimizing numerical artifacts without compromising a smooth transition in vertical coordinate thickness.

4. Cold-start RAP simulations

Once the hybrid, terrain-following coordinate was successfully integrated into the WRF code repository within GSD, initial testing began with a number of cold-start simulations within the RAP model. These cold-start cases served as a first attempt to analyze the behavior of the hybrid terrain-following coordinate, ensuring that its implementation within the model was successful and offering a controlled environment to compare it to the traditional, sigma terrain-following coordinate. Therefore, two identical simulations were conducted per case, with the only difference being the vertical coordinate (one simulation using the hybrid, and the other with the sigma, terrain-following coordinate). Each simulation began with a Global Forecast System (GFS) analysis that was downscaled to the 13-km RAP grid. The RAP was then initialized from this downscaled state, without using data assimilation. After running through a digital filter initialization (Peckham et al. 2016), a 24-h free forecast was run. Boundary conditions were created with forecasts from the same GFS cycle used for the initialization. To summarize the main findings from these tests, three sets of simulations will be described: two single initialization forecasts starting at 0000 UTC 7 March 2017 and

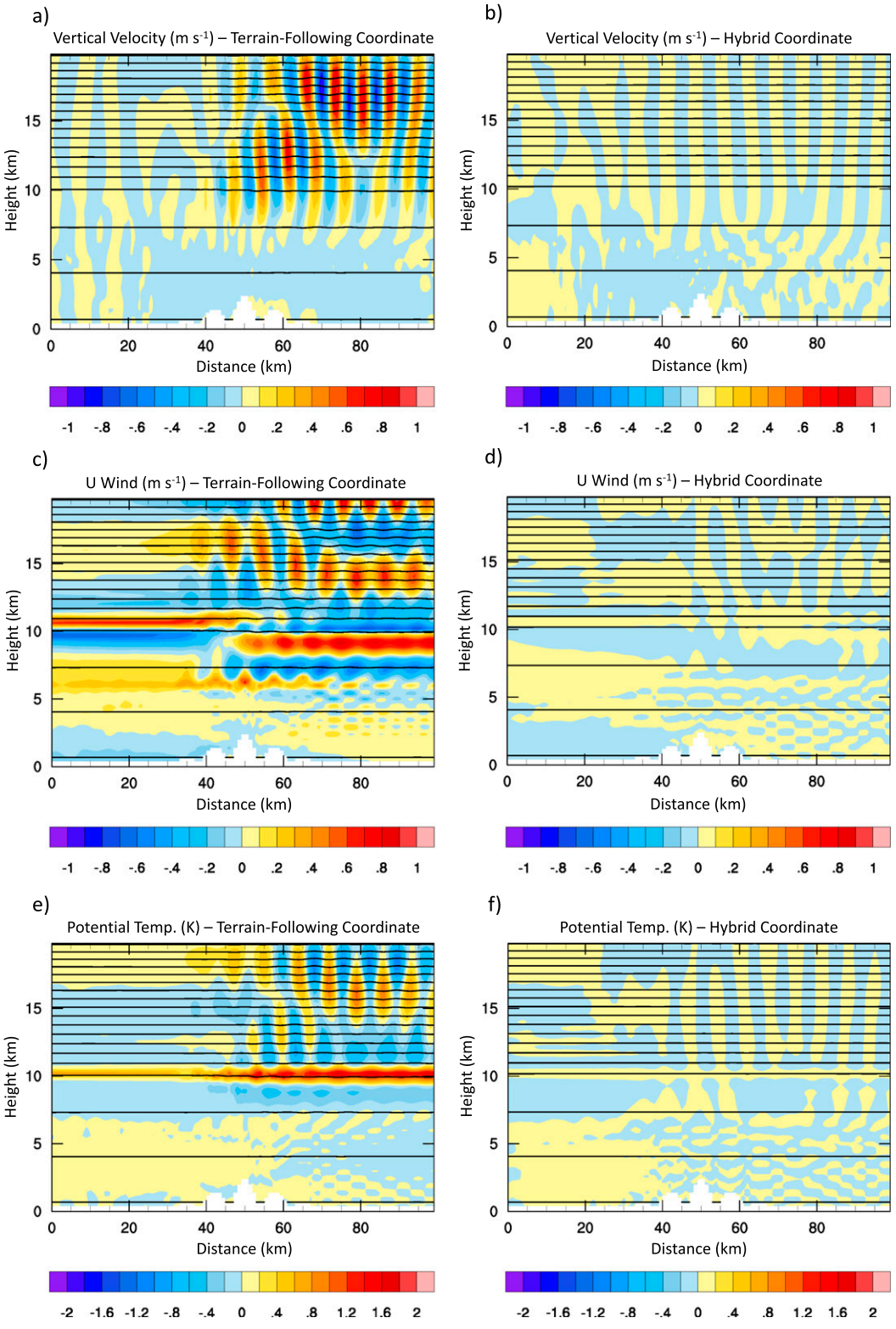

FIG. 2. Idealized advection simulation results using the (left) sigma, terrain-following coordinate and (right) hybrid coordinate for (a),(b) vertical velocity ($m\,s^{-1}$) at 5 h into the forecast, (c),(d) *U* wind component ($m\,s^{-1}$) differences between initialization and the 5-h forecast, and (e),(f) potential temperature (K) differences between initialization and the 5-h forecast. Potential temperature contours are shown in black from 290 to 460 K in intervals of 10 K.

at 1200 UTC 17 November 2016, followed by a week-long set of cold-start simulations between 7 and 13 March 2017. These particular time periods were chosen due to strong west and northwesterly flow across the Rocky Mountains, ideal for vertically propagating mountain wave formation, and representing synoptic patterns in which the hybrid coordinate was expected to provide a positive impact.

a. 7 March 2017

Since the sigma, terrain-following coordinate is known to impart artificial accelerations/decelerations into the model equations, initial analysis was focused on the wind field of the RAP cold-start simulations to assess differences between the two coordinates. For the first set of these simulations, initialized at 0000 UTC 7 May 2017, a long-wave trough was situated over the western two-thirds of the United States (Fig. 3a). The axis of strongest winds was located over the Pacific Northwest into the Central Plains region, with wind speeds approaching 150 kt (1 kt $\approx$ 0.51 m s^{-1}) in several locations. Corresponding wind field differences between simulations using the sigma, terrain-following and hybrid coordinates at 250 hPa are also shown for the initialization (Fig. 3b), 6-h (Fig. 3c), and 12-h forecasts (Fig. 3d) over the full North American domain.

At initialization (Fig. 3b), only very minor differences can be seen between the simulations, concentrated over small areas of Mexico, Nevada–Utah, and Colorado. Adjacent to or within complex terrain, these regions contain interpolation differences during the generation of initial conditions from the GFS. As the forecast progresses, more discrepancies between the coordinates are apparent by 6 h (Fig. 3c). Marked differences are apparent along the main jet axis from Washington State, southeastward toward Kansas, where the forecast winds using the hybrid coordinate are notably stronger than those produced when using the sigma, terrain-following coordinate. As the hybrid coordinate reduces spurious noise in all directions, mixing of horizontal momentum in this jet axis was reduced with the hybrid coordinate, resulting in stronger flow than is seen with the pure sigma coordinate. At 12 h into the forecast (Fig. 3d), differences found over mountainous regions during the 6-h forecast have now been advected downstream to regions in the central United States, parts of Canada, the Gulf of Alaska, and Central America. Differences in wind speed between the two coordinates reached upward of 14 kt over western Kansas, at the base of the main longwave trough over the United States.

In general, the 7 March 2017 cold-start RAP comparisons revealed that the majority of wind speed differences were focused over or downwind of major mountain ranges, specifically in the western areas of North America. These impacts were then advected downstream as the forecast progressed. As expected, no differences were found to occur well away from land, such as over the Pacific Ocean, or in areas not downwind of complex terrain.

b. 17 November 2016

The second set of simulations was initialized at 1200 UTC 17 November 2016 in order to assess the impact of the hybrid vertical coordinate on the vertical structure of mountain waves and artificial noise over the Rocky Mountain region of the United States. Figure 4 shows a west–east cross section from California to Colorado of vertical velocity (color) and potential temperature (contoured) for the 5-h forecast from this case. Horizontal wind vectors are also shown, indicating a trough was present over the western United States. With the resulting flow pattern providing a favorable environment for mountain wave development, vertically propagating waves are apparent in the vertical velocity field.

In the terrain-following sigma coordinate (Fig. 4a), vertical motion is being generated by a combination of true mountain wave development and artificial noise, generated by the coordinate itself. A delineation between the two is possible, based on the assumption that, without wave breaking aloft, physically realistic mountain waves tilt upwind with height in the simulation, consistent with upwind propagation of energy. Given this expected behavior, most features positioned between 900 and 1500 km (x axis) and from 2 to 6 km in height (y axis) above mean sea level (MSL) are believed to be genuine (Fig. 4a), whereas the perfectly vertical structures apparent above the Sierra Nevada mountains (200–300 km) are artifacts of the terrain-following, sigma coordinate. In Fig. 4b, the assumed spurious vertical motions generated by the traditional sigma coordinate have been largely removed, while the actual vertically propagating mountain waves are still present. In addition, the mountain waves exhibit more coherent structure and upwind tilt without the contamination of artificial noise.

c. 7–13 March 2017

A more quantitative verification approach was undertaken with a series of cold-start simulations between 7 and 13 March 2017. These simulations followed the same methodology as the previous cold-start forecasts, with interpolation of downscaled GFS data that was run through a digital filter prior to model integration, but additionally allowed for an assessment of the two

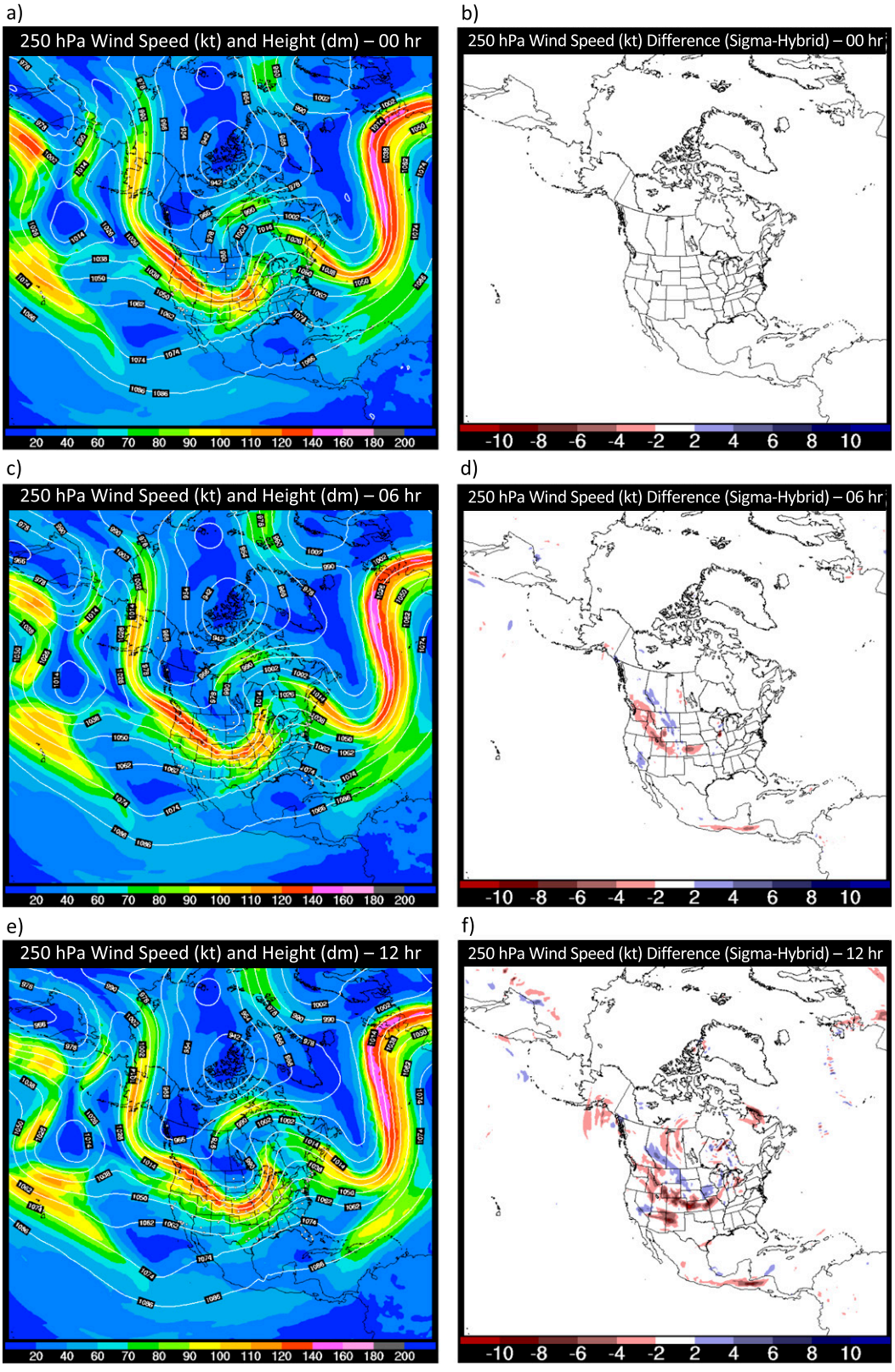

FIG. 3. Sigma, terrain-following cold-start RAP simulation plots of 250-hPa wind speed (kt) and geopotential heights (dam), and wind speed (kt) difference plots between the two coordinate simulations (sigma − hybrid) for model forecasts initialized at 0000 UTC 7 Mar 2017. (a),(c),(e) Initialization, 6-, and 12-h forecasts and (b),(d),(f) differences are shown.

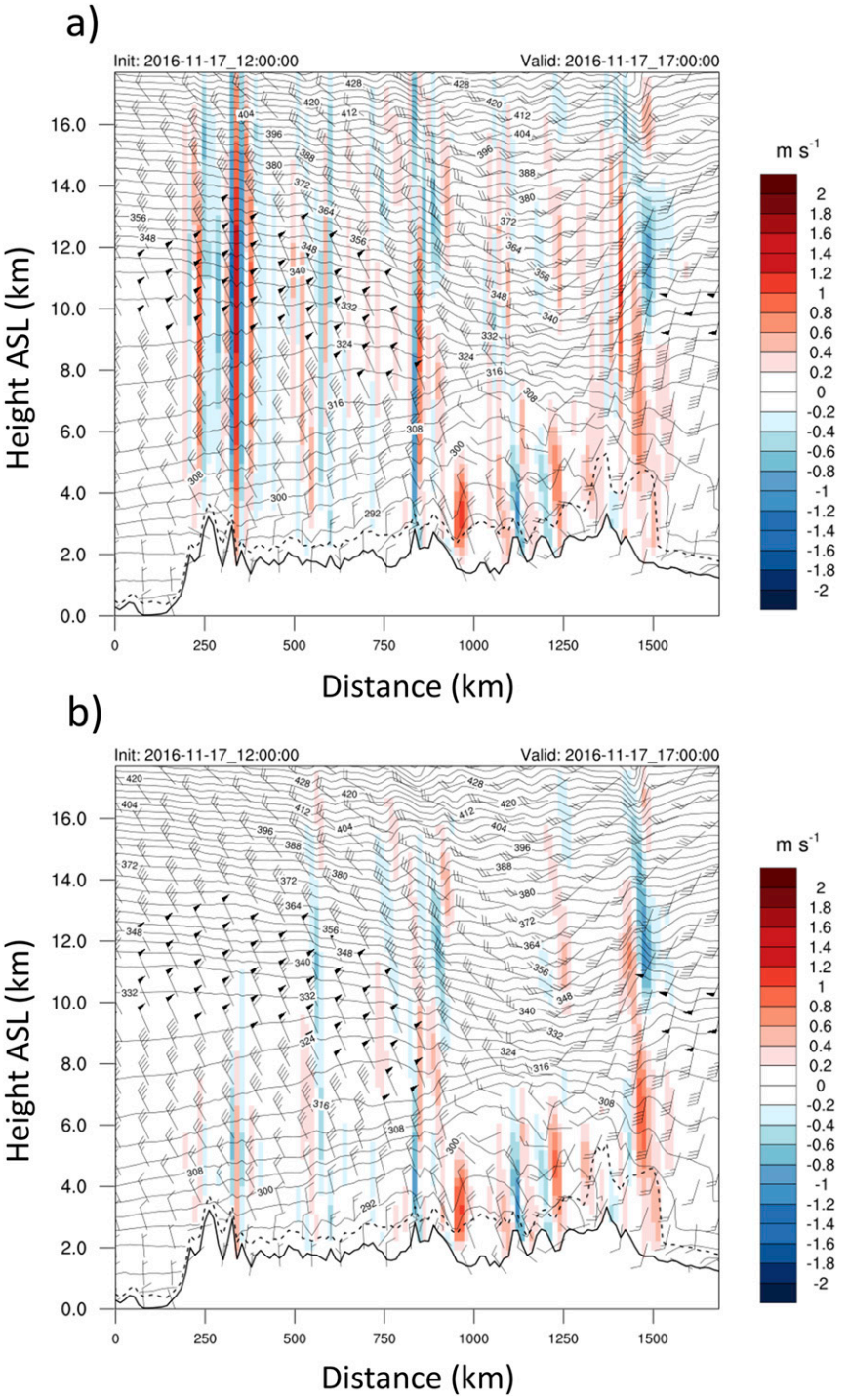

FIG. 4. Cross-section plots of vertical velocity (color), potential temperature (contours), and horizontal wind vectors ($m\,s^{-1}$) for 5-h RAP model forecasts, initialized at 1200 UTC 17 Nov 2016, using (a) the original sigma, terrain-following coordinate and (b) the new hybrid vertical coordinate. The top of the planetary boundary layer is shown as a dashed line with topography shown in solid black. Both cross sections represent a vertical slice from California to Colorado, from left to right.

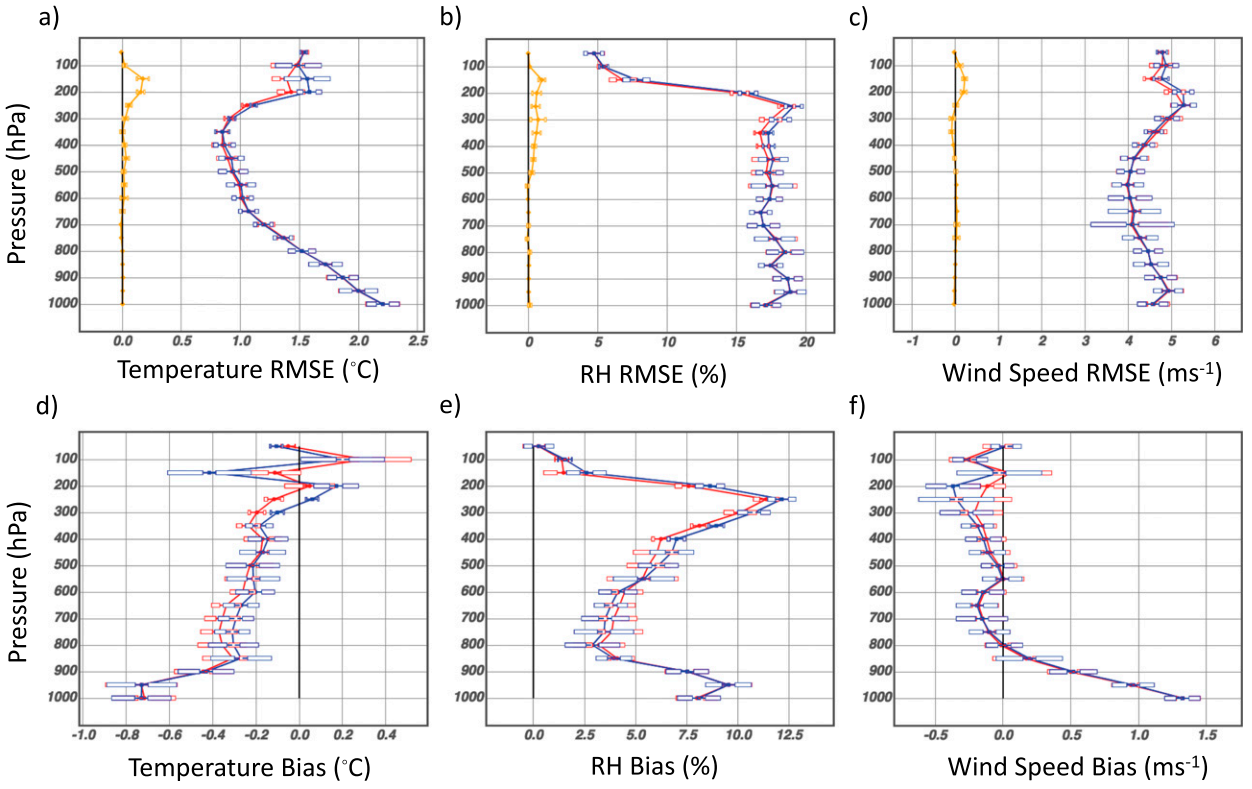

FIG. 5. Vertical profiles of average (top) RMSE and (bottom) bias for 12-h forecasts of (a),(d) temperature (°C), (b),(e) relative humidity (%), and (c),(f) wind speed ($m\,s^{-1}$) for cold-start RAP simulations initialized at 0000 UTC between 7 and 13 Mar 2017, as compared to rawinsonde observations. Red lines correspond to the hybrid vertical coordinate simulations, while blue lines represent the original sigma vertical coordinate simulations. Orange lines in the RMSE plots show the difference between the two (sigma − hybrid). Confidence intervals (95%) are shown as boxes on the lines for each vertical level.

vertical coordinates across the full RAP domain and over a number of different initializations. Forecasts were initialized every day at 0000 UTC, followed by post processing with the unified post processor (UPP) to generate standard output fields in grib2 format and verification using the Model Analysis Tool Suite (MATS) from ESRL/GSD (Smith et al. 2019). Domainwide, averaged root-mean-square error (RMSE) and bias of temperature, relative humidity, and wind speed for all 12-h forecasts were calculated using available CONUS rawinsonde data from the same period (Fig. 5). Statistical significance bars were generated every 50 hPa in pressure, using a single standard deviation from the mean with a correction applied for autocorrelation (Weatherhead et al. 1998).

Results from this series of cold-start simulations show that most of the impact of switching to the hybrid vertical coordinate is concentrated in the upper levels of the atmosphere, suggesting that improvements from the hybrid coordinate are sensitive to the jet-level flow for a given retrospective period. In particular, statistically significant pairwise differences exist (errors bars do not encompass zero) for temperature and wind speed (Figs. 5a,c) above ~300 hPa when the hybrid coordinate is employed. For relative humidity (Fig. 5b), statistically significant improvements (based on pairwise differences) in RMSE can be seen above ~500 hPa. Corresponding improvements in bias are also seen for these same levels in Figs. 5d–f. While some degradation in bias is found at lower levels for temperature bias (Fig. 5d) and relative humidity (Fig. 5e), these differences are not statistically significant.

5. Week-long, retrospective simulations

While the cold-start RAP simulations provided valuable insight into differences between the two vertical coordinates, testing of the hybrid coordinate within the operational configurations of both the RAP and HRRR (including the critical data assimilation component) is essential to understanding the cumulative, long-term impacts of the hybrid vertical coordinate over many forecasts. To this end, two sets of week-long retrospective simulations were designed to assess the hybrid

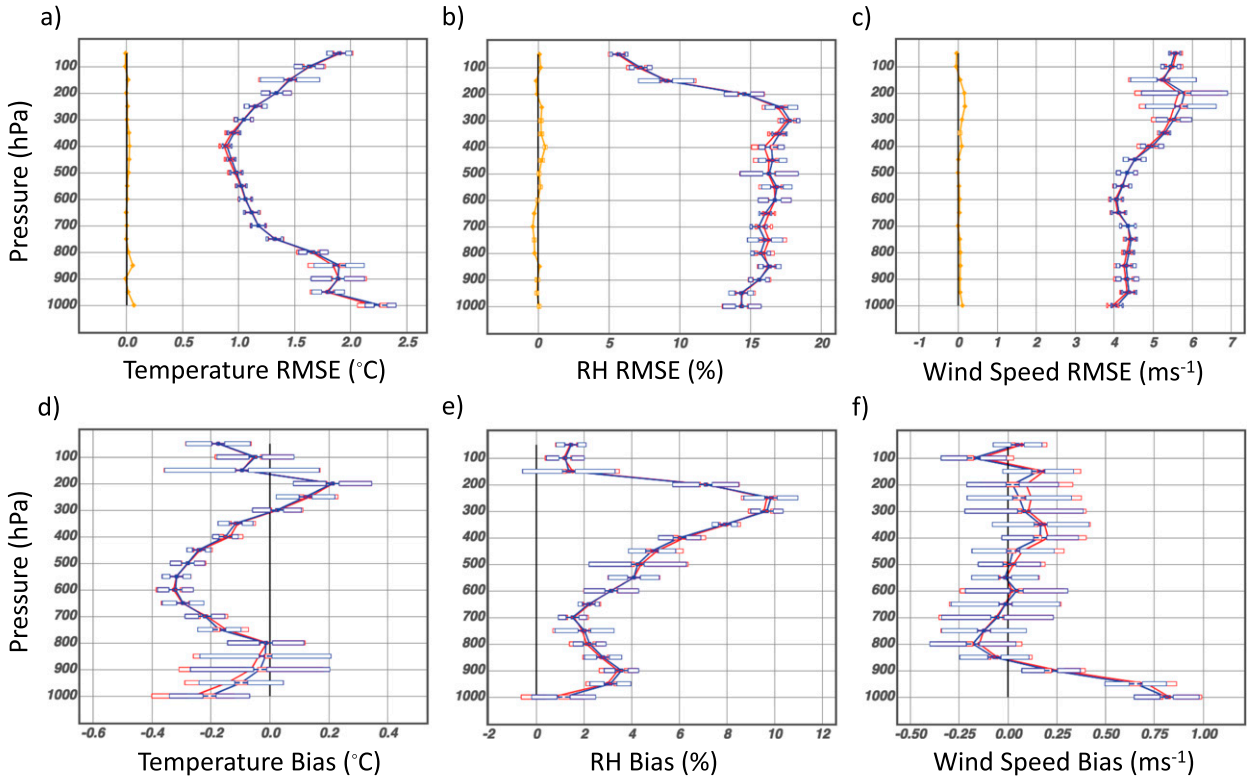

FIG. 6. Vertical profiles of average (top) RMSE and (bottom) bias for 12-h forecasts of (a),d) temperature (°C), (b),(e) relative humidity (%), and (c),(f) wind speed ($m\,s^{-1}$) from fully cycled RAP simulations initialized every hour between 1200 UTC 1 Jan and 0000 UTC 8 Jan 2017, as compared to rawinsonde observations. Red lines correspond to the hybrid vertical coordinate simulations, while blue lines represent the original sigma vertical coordinate simulations. Orange lines in the RMSE plots show the pairwise differences between the two coordinates (sigma − hybrid). Confidence intervals (95%) are shown as boxes on the lines for each vertical level.

coordinate: one from 1 to 7 January 2017 for the RAP, and the other from 3 to 10 September 2016 for the HRRR. As with the cold-start cases, the only difference between the simulations in each set of experiments was the type of vertical coordinate employed: sigma, terrain-following or hybrid. Upon completion, bias and RMSE vertical profiles of standard variables were once again verified against upper-air soundings.

a. RAP retrospective simulations

To run the cycled RAP simulations, an end-to-end workflow was created to be identical to the operational implementation of the RAP, as outlined in Benjamin et al. (2016). Each simulation was initialized through data assimilation conducted directly on the sigma, terrain following or native hybrid coordinates, followed by application of a digital filter. After initialization, free forecasts of the RAP were run out to 18 h, with the 1-h forecast used as the background for the following cycle, except during partial cycling periods [Fig. 2 from James and Benjamin (2017)]. Forecasts were then postprocessed through UPP and verified using MATS. As in the cold-start simulations, vertical profiles of averaged, domainwide RMSE and bias were produced for 12-h forecasts from both simulations (Fig. 6).

Results from these vertical profiles indicate that minor improvements in RMSE were found for temperature (Fig. 6a), relative humidity (Fig. 6b), and wind speed (Fig. 6c), with the largest impact occurring aloft for wind speed. In some cases, the pairwise differences indicate statistically significant improvements for the hybrid coordinate at certain isobaric levels, specifically for relative humidity at 400 hPa and wind speed near 250 hPa. Yet, a slight degradation in relative humidity is also found to be statistically significant around 700 hPa. All three variables show minor reductions in RMSE near the surface for the hybrid coordinate, indicating that improvements are not solely confined to the upper levels. Only very minor differences are found when looking at the biases between the two vertical coordinate simulations (Figs. 6d–f), with a slight increase in bias for temperature near the surface (Fig. 6d) and wind speed aloft (Fig. 6e) when using the hybrid coordinate.

It is interesting to note that aside from upper-level wind speed comparisons, the differences in RMSE and bias between the two vertical coordinates are generally larger in the cold-start RAP simulations than in the hourly cycled, week-long RAP retrospective runs. One potential explanation for these differences is related to the hybrid ensemble–variational data assimilation aspect of the week-long, cycled simulations. Since the dry hydrostatic pressure determines the height of the vertical coordinate surfaces, changes in mass distribution introduced through analysis increments will directly impact the vertical distribution of the hybrid coordinate levels. Therefore, it is possible that GSI is not optimizing these vertical coordinate locations, particularly in complex terrain. As a result, improvements with the hybrid coordinate could be minimized when compared to the sigma, terrain-following coordinate. Further testing is required to investigate this hypothesis.

Another possibility is related to the synoptic differences between the retrospective periods chosen for the cold-start and fully cycled simulations. The cold-start runs from 7 to 13 March 2017 featured a long-wave trough across much of the CONUS, with persistent northwesterly flow over the intermountain West, while the 1–7 January 2017 period was dominated by westerly flow aloft, with only weak northwesterly flow at the very end of the period. This lack of northwesterly flow during the January retrospective period is not as conducive to vertically propagating mountain waves and may have limited the improvement of the hybrid vertical coordinate over the sigma, terrain-following coordinate during the fully cycled set of simulations. These synoptic differences are also manifested when comparing the vertical profile verification plots between the cold-start and cycled experiments, as it is clear that the error statistics are not the same, particularly when looking at the magnitude of RMSE and bias.

b. HRRR retrospective simulations

For the week-long HRRR simulations, another end-to-end workflow was created, with similar components to those used during the week-long RAP simulations. However, the 3-km HRRR differs from the RAP in a number of major ways. First, it is not a fully cycled system, instead relying hourly on the downscaled 13-km RAP initialization, which is interpolated to a 3-km grid. Then, a 1-h preforecast is conducted, where 15-min reflectivity fields are used to generate temperature tendencies applied at each minute of the preforecast. The goal of these temperature tendencies is to spin up convective-scale vertical motions through the application of latent heating in regions of observed reflectivity. After this preforecast concludes, hybrid EnKF–variational data assimilation is conducted using the GFS ensemble and traditional observations, followed by a nonvariational GSI cloud analysis step, similar to the RAP. A 24-h free forecast is then issued, with the land surface state from initialization used in the subsequent cycle of the HRRR.

Verification of RMSE for temperature (Fig. 7a), relative humidity (Fig. 7b), and wind speed (Fig. 7c) indicate very little difference between the sigma, terrain-following and hybrid coordinates with the HRRR week-long simulations. Most differences are small and insignificant, aside from near 100 hPa for all three variables. A similar lack of differences can be seen in the bias plots (Figs. 7d–f), with none of the pairwise differences being statistically significant aside from at 100 hPa for temperature (Fig. 7d), where the sigma, terrain-following coordinate exhibits a slightly lower bias.

Since the HRRR is not a fully cycled model, and inherits its initial background field from the downscaled RAP, any differences between the two vertical coordinates that are generated at 3 km are unable to be maintained from cycle to cycle. In addition, both of the week-long, vertical coordinate simulations within the HRRR used the same sigma, terrain-following RAP simulation as a model background, potentially further limiting the ability of the HRRR to produce differences between vertical coordinate simulations. Finally, since the HRRR uses the same hybrid ensemble–variational data assimilation as the RAP, suboptimal placement of the vertical coordinates based on analysis increments is possible in complex terrain.

The upper-level flow during the 3–10 September 2016 retrospective period may be an additional reason for the lack of differences between the vertical coordinates in the HRRR. With few synoptics systems moving through the domain, much of the period was dominated by zonal, relatively weak upper-level winds. In addition, this lack of strong upper-level flow was not conducive to vertically propagating mountain waves. Given this synoptic pattern, the atmosphere likely lacked sufficiently strong pressure gradients for the hybrid coordinate to improve numerical truncation errors over complex terrain, and thus any improvements over the sigma, terrain-following coordinate were limited.

6. HRRR case study

In a similar manner to the cold-start RAP tests, a few single-initialization HRRR simulations were run within the DTC to conduct time series and vertical profile verification using the Model Evaluation Tools (MET) verification package. Plots of spatial cross sections of the domain to assess differences when using the hybrid versus sigma, terrain-following coordinate were also

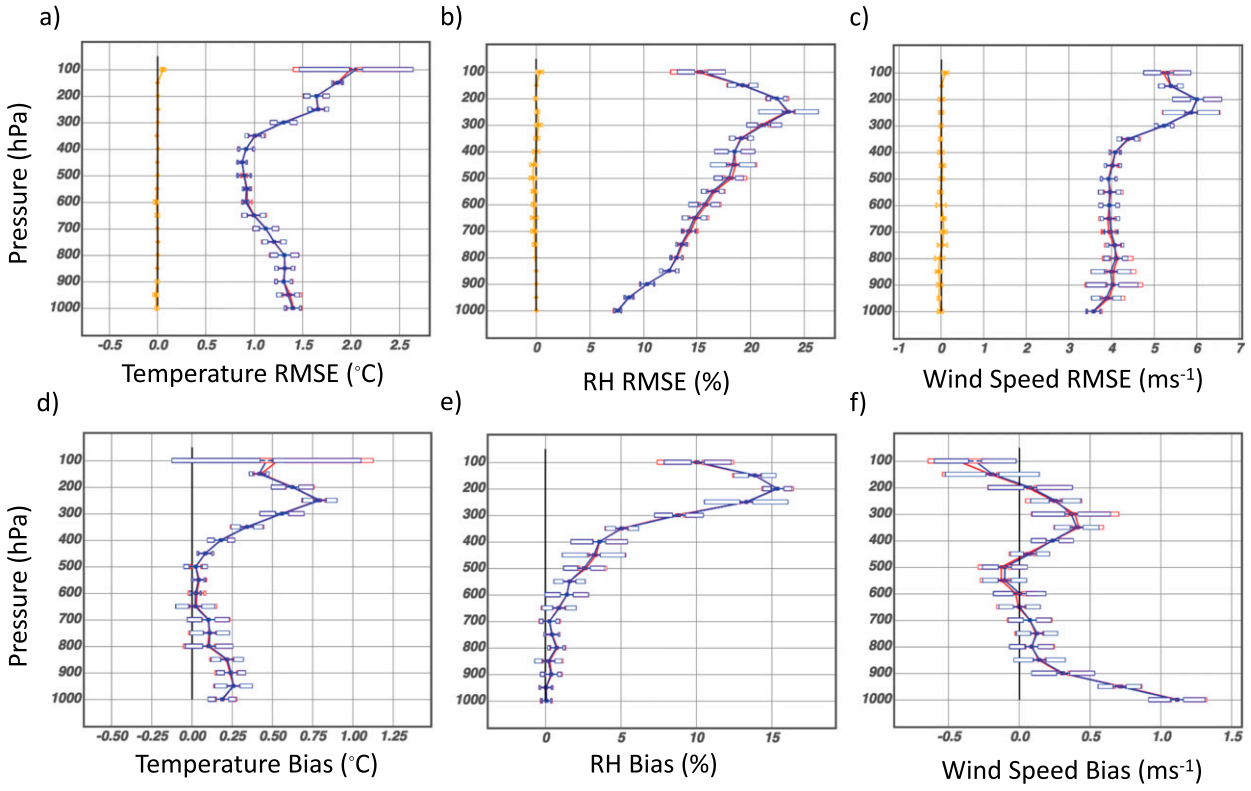

FIG. 7. Vertical profiles of average (top) RMSE and (bottom) bias for 12-h forecasts of (a),(d) temperature (°C), (b),(e) relative humidity (%), and (c),(f) wind speed ($m\,s^{-1}$) for HRRR forecasts initialized every hour between 0000 UTC 3 Sep and 0000 UTC 10 Sep 2016, as compared to rawinsonde observations. Red lines correspond to the hybrid vertical coordinate simulations, while blue lines represent the original sigma vertical coordinate simulations. Orange lines in the RMSE plots show the pairwise differences between the two coordinates (sigma − hybrid). Confidence intervals (95%) are shown as boxes on the lines for each vertical level.

generated. One of the periods chosen for these simulations was from 8 to 9 May 2016, when diffluent upper-level flow associated with a cutoff low over the central Rocky Mountains aided in the development of numerous severe thunderstorms from Texas to Nebraska. To assess the impact of the hybrid vertical coordinate for this period, two cold-start HRRR simulations were conducted at 0000 and 1200 UTC 9 May 2016, with the HRRR being initialized from the downscaled RAP analysis at the same time, followed by a free forecast out to 24 h. No preforecast or data assimilation was conducted for this case study.

With verification from the week-long HRRR retrospective simulations showing little difference between the vertical coordinates, it may be tempting to suppose that individual forecast vertical profile verification would result in similar findings. However, as can be seen for the 12-h HRRR forecast from 0000 UTC 9 May 2016 (Fig. 8), a number of notable differences exist between the two vertical coordinates. In general, RMSE is slightly lower for midtropospheric temperature (Fig. 8a) and for wind speed below the tropopause (Fig. 8e) for the hybrid coordinate simulation, while neither vertical coordinate shows a systematic improvement for dewpoint temperature (Fig. 8c). In addition, bias is lower when using the hybrid vertical coordinate for both temperature (Fig. 8b) and dewpoint temperature (Fig. 8d) above 700 hPa. Vertical profiles of wind speed bias (Fig. 8f) did not show a clear indication that either vertical coordinate performed better than the other.

In addition to vertical profile verification for the 9 May 2016 simulations, spatial plots were generated at specific isobaric levels to evaluate qualitative differences between the two vertical coordinates for measures such as relative humidity, wind speed, vertical velocity, temperature, and composite reflectivity. Figures 9a and 9b illustrate the 12-h forecast differences for relative humidity at 500 hPa (Fig. 9a) and 250-hPa wind speed (Fig. 9b) over the CONUS domain. Figure 9c shows the 12-h forecast composite reflectivity from the case study experiment using the hybrid coordinate, while the corresponding composite reflectivity for the simulation using the sigma, terrain following coordinate is displayed in Fig. 9d.

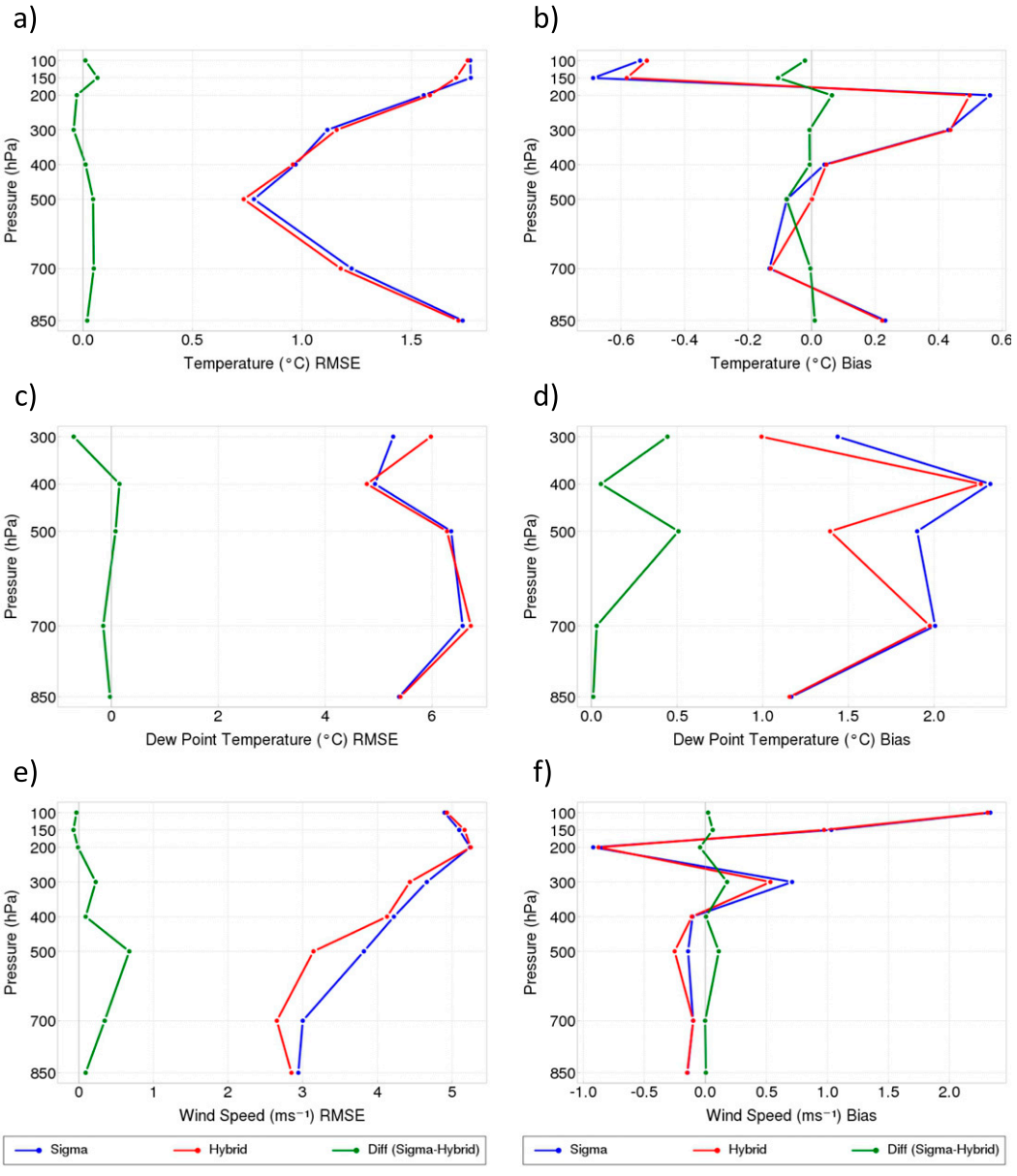

FIG. 8. Vertical profiles of average (left) RMSE and (right) bias for (a),(b) temperature (°C), (c),(d) dewpoint (°C), and (e),(f) wind speed ($m\,s^{-1}$) for 12-h HRRR forecasts initialized at 0000 UTC 9 May 2016, as compared to rawinsonde observations. The hybrid vertical coordinate simulation is shown in red, while the sigma, terrain-following coordinate is shown in blue. The pairwise differences between the two coordinates (sigma − hybrid) are shown in green.

Figures 9a and 9b show the immediate impact of the hybrid vertical coordinate both over and downwind of the complex terrain of the Rocky Mountains. In particular, most of the differences were associated with the convection (and potentially the placement of individual convective storms) occurring over the Plains during this period; however, impacts on relative humidity at 500 hPa (and to a lesser extent, 250-hPa wind speed) can be seen over the higher terrain of Utah and Colorado, extending northwestward. In addition, the 250-hPa wind speed spatial plot indicates that the location and intensity of convective updrafts were likely displaced from one vertical coordinate to the other, demonstrated by concentric bands of weaker and stronger wind speeds at various locations. Differences in gravity wave activity emanating from the anvils of the convective storms is likely responsible, due to disparity in location and timing of convection.

The verification profiles and spatial plots from 9 May 2016 indicate that the choice of vertical coordinate

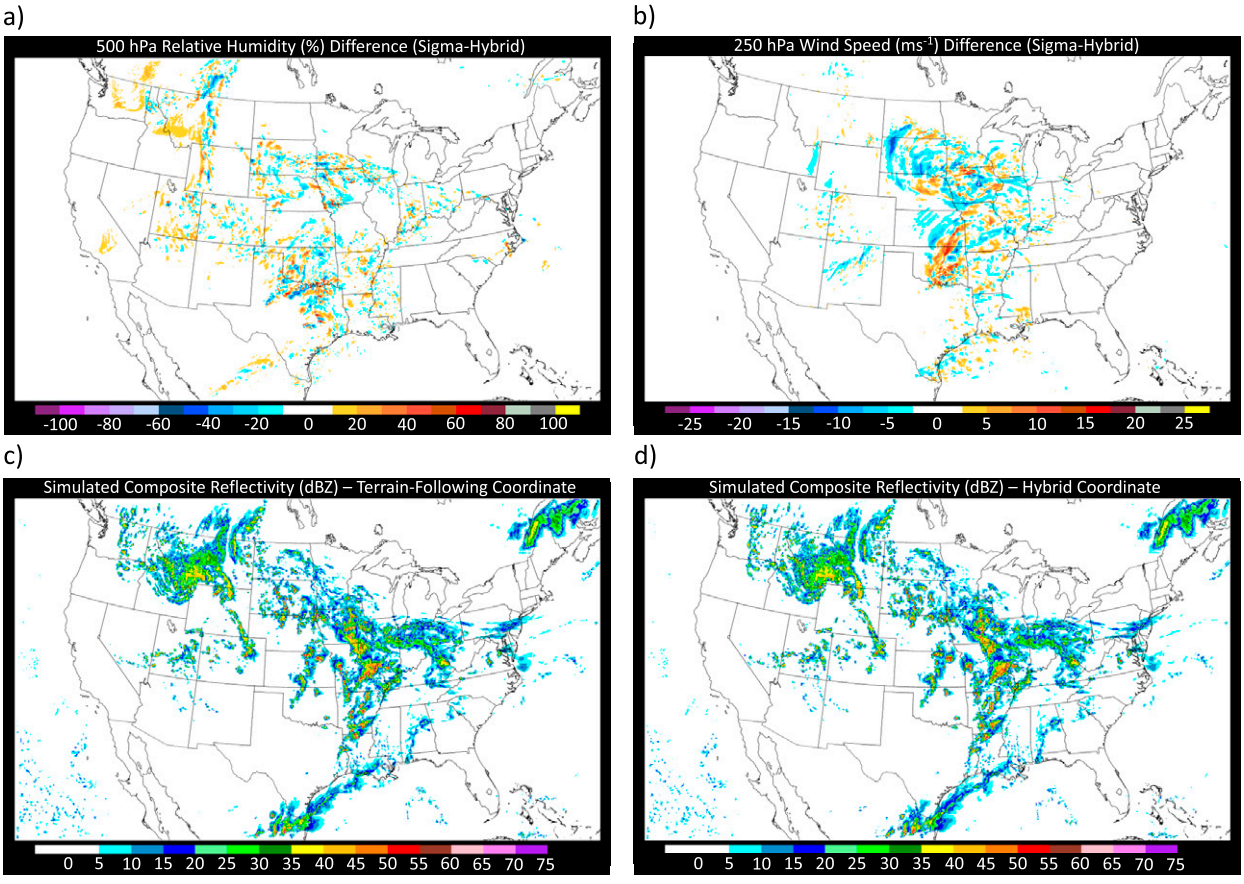

FIG. 9. The 12-h forecast difference plots of (a) 500-hPa relative humidity and (b) 250-hPa wind speed from two HRRR simulations (hybrid − sigma), initialized at 0000 UTC 9 May 2016, with (c) a sigma-terrain following coordinate plot of composite reflectivity and (d) corresponding hybrid coordinate plot of composite reflectivity. Cool colors indicate drier relative humidity in (a) and weaker wind speed values in (b) for the hybrid coordinate.

is indeed producing divergent model solutions in the HRRR, contrary to what might be inferred from the week-long HRRR retrospective runs. The HRRR case study suggests the possibility that verification differences between the vertical coordinate solutions may potentially be washed out when aggregated over a longer period of time, assuming the observed divergence in solutions is not systematic. It is also possible that data assimilation, which is not used in the HRRR case study, may be reducing the impact of the hybrid vertical coordinate in the week-long simulations, as discussed previously. Specifically for the 9 May 2016 simulations, the proximity of the severe weather outbreak to the higher terrain to the west likely influenced the differences seen between the two vertical coordinates, as model variability from using the two vertical coordinates interacted with the development of convection. In addition, qualitative comparisons of the spatial plots reveal that variability between the two coordinates is maximized near areas of inclement weather, while regions without convection show little difference. Both the vertical profile verification and the spatial plots provide a detailed look into the run-to-run variability between model solutions that is nearly imperceptible when analyzing a week-long retrospective simulation where data are aggregated over a long period of time.

7. RAP turbulence forecasting

Output from the RAP and HRRR is also utilized extensively within the aviation industry. As part of a suite of related forecast guidance, the NOAA Aviation Weather Center (AWC) produces operational turbulence intensity forecasts, or graphical turbulence guidance (GTG), from the surface up to 45 000 ft MSL, derived from postprocessed RAP model data (Sharman et al. 2006). However, due to the use of the sigma, terrain-following vertical coordinate in the WRF Model, artificial wind field disturbances (and thus vertical motion) have made AWC forecasts of mountain wave–associated

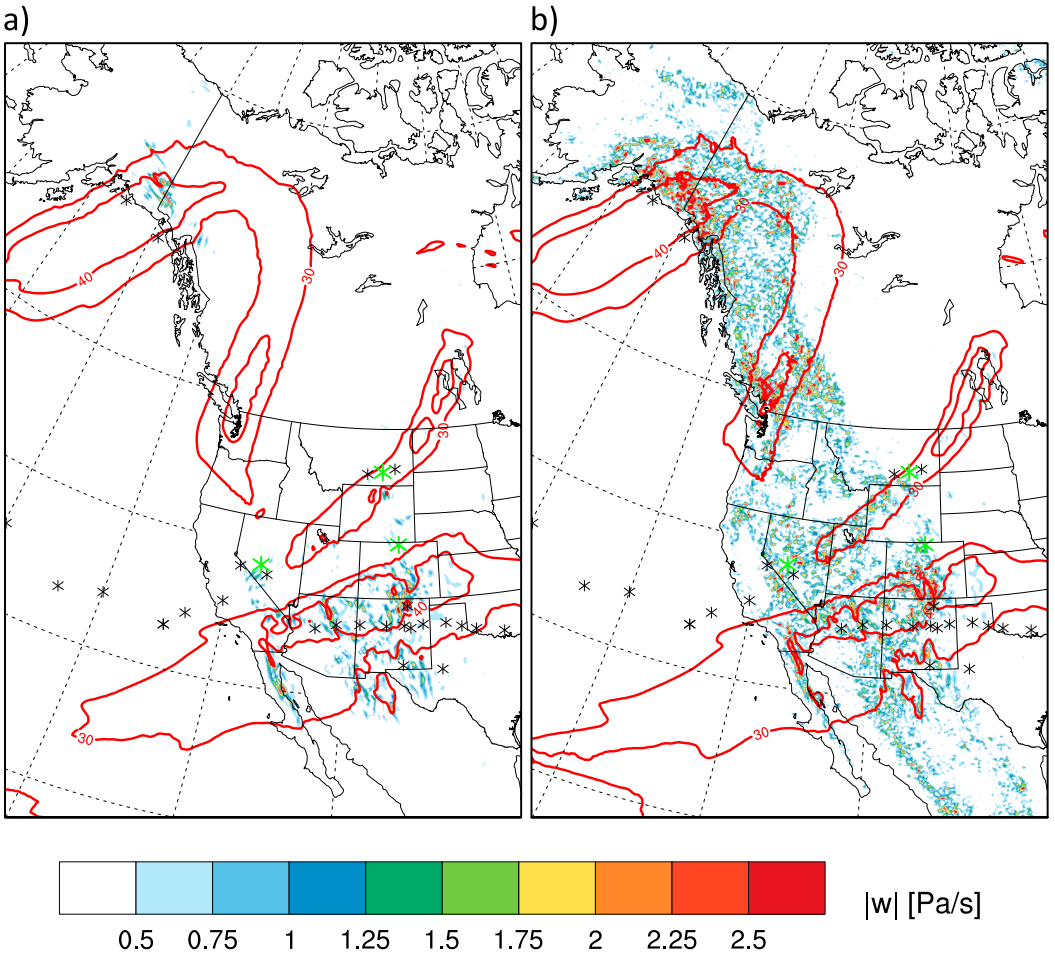

FIG. 10. RAP 6-h forecasts of absolute vertical motion $|w|$ (in color) with horizontal wind speed (contoured at 30 and 40 m s^{-1}) for 35 000 ft above mean sea level over western North America valid at 1800 UTC 25 May 2017, using (a) the hybrid vertical coordinate (from the GSD RAP), and the (b) sigma, terrain-following coordinate (from the NCEP RAP) (adapted from Kim et al. (2019), Fig. 3). Pilot reports for smooth (turbulence intensity of zero) and rough (turbulence intensity ≥ 2) conditions are shown in black and green stars, respectively. Reports were made within a ±2-h window of 1800 UTC and ±1000 ft of 35 000 ft above mean sea level.

turbulence prone to unrealistically large values, particularly over western regions of North America.

In an attempt to improve GTG, an analysis was conducted to test the impact of the hybrid vertical coordinate on turbulence forecasts issued for aircraft near a cruising altitude of 35 000 feet above mean sea level (Kim et al. 2019). Prior to its official implementation, the hybrid vertical coordinate was included in a real-time version of the RAP at GSD, making it possible to source output from both the operational NCEP RAP (using the sigma, terrain-following coordinate) and this newly configured parallel version running with the hybrid vertical coordinate. Once data were postprocessed using the AWC turbulence algorithm, results were compared between the two RAP implementations to assess the location and breadth of turbulence. Finally, pilot-reported regions of turbulence were overlaid to assess the ability of the hybrid coordinate–based simulations to detect areas of authentic turbulence.

Figure 10 shows 6-h forecast plots of absolute vertical motion at 35 000 feet above mean sea level in color, with contours of horizontal wind speed in red. It is clear from comparing the turbulence forecasts using data from the NCEP RAP and the GSD RAP, that the sigma, terrain-following vertical coordinate is producing broad areas of artificial vertical motion over much of the Rocky Mountains, from Alaska to Mexico (Fig. 10b). In contrast, areas of spurious vertical motion are drastically reduced in the GSD RAP, with the remaining regions of vertical motion confined to areas of high horizontal wind speeds. Pilot reports of turbulence also indicate that the vertical motion derived from the GSD RAP data is much more reliable than that from the NCEP RAP, further validating the use of the hybrid vertical coordinate.

Improvements seen within the idealized (Fig. 2) and RAP cold-start (Fig. 4) simulations illustrate the advantage of adopting the hybrid coordinate on mesoscale phenomena, such as mountain waves, while Fig. 3 shows the impact on synoptic-scale upper-level winds. The GTG forecast improvements are also manifestations of a reduction in wind field disturbances, just on a smaller scale. As such, benefits from the hybrid vertical coordinate are fully consistent across these scales.

8. Summary and conclusions

GSD conducted extensive testing of the newly developed, WRF-based hybrid coordinate through a number of simulations within the RAP and HRRR models. Experiments within the RAP began with cold-start simulations with and without the new hybrid coordinate to isolate impacts on upper-air variables and mountain-wave features. Week-long, fully cycled retrospective simulations were then run for both the RAP and HRRR to test the new vertical coordinate in an operationally identical environment. Finally, cold-start HRRR case study analyses were conducted by the DTC to assess the impacts of the hybrid vertical coordinate on traditional vertical profiles as well as spatial patterns across the domain. Major conclusions from these experiments are listed below:

- Cold-start RAP simulations identified localized impacts of the hybrid vertical coordinate downwind of major areas of complex terrain, with reduced spurious noise and more coherent mountain wave features.
- Vertical profile verification of cold-start RAP simulations showed upper-level RMSE improvements when using the hybrid vertical coordinate, while the week-long, cycled operational RAP and HRRR retrospective tests indicated only nonstatistically significant differences between the two coordinates.
- Single-initialization HRRR case studies illustrated localized variability between model simulations using the two vertical coordinates, with maximum differences occurring in regions where turbulent or convective events were occurring. Downstream advection of these differences was also apparent in each case.
- Turbulence forecasts using the RAP were improved through the implementation of the hybrid coordinate, drastically reducing spurious vertical wind field disturbances that were previously seen when using the sigma, terrain-following coordinate.

Hybrid coordinate improvements identified in the cold-start RAP simulations did not translate to the vertical profile verification of the week-long, fully cycled RAP and operational HRRR simulations. Neither vertical coordinate was statistically better than the other for the fully cycled experiments when assessing vertical profiles of temperature, relative humidity, or wind speed. It is possible that the addition of data assimilation may minimize the benefits of the hybrid vertical coordinate through suboptimal placement of vertical coordinate surfaces in both the RAP and HRRR. Successive implementation of analysis increments in complex terrain that sufficiently displace vertical surfaces would reduce any improvements from use of the hybrid vertical coordinate in previous cycles.

While objective verification from the cycled, week-long simulations showed minimal differences between the two vertical coordinates, vertical cross-section and spatial plots from the cold-start simulations of the RAP and HRRR indicate that large differences in upper-level variables are apparent and are advected downstream from complex terrain. In some of the HRRR case studies, discrepancies between the two vertical coordinates can be found as far east as the Atlantic Ocean at longer forecast hours. In addition, the fact that these differences also appear in the vertical profile verification from the HRRR case studies may lend credence to the possibility that data assimilation is limiting the positive impacts of the hybrid vertical coordinate within the operationally similar HRRR experiment.

The vertical cross-section plots of the cold-start RAP simulations as well as AWC turbulence forecasting also demonstrate the importance of the hybrid vertical coordinate in reducing artificial horizontal and vertical accelerations/decelerations in the wind field, reducing spurious noise in the model forecasts. It is possible that these types of small-scale improvements are too localized to be represented in the synoptic-scale vertical profile verification, another potential reason why more improvement is not seen in the week-long retrospective simulations. Further investigation into these apparent small-scale improvements, as well as the impact of data assimilation and cycling on model simulations using the hybrid vertical coordinate are warranted to improve understanding of its impact on mesoscale simulations.

Acknowledgments. Thanks are due to Jeff Hamilton and Molly Smith for their help with MATS. This research was supported by NOAA Award NA14OAR4320125. Jung-Hoon Kim was supported by the Basic Science Research Program through the National Research Foundation of Korea (NRF), funded by the Ministry of Education (NRF-2019R1I1A2A01060035).

REFERENCES

Benjamin, S. G., and Coauthors, 2016: A North American hourly assimilation and model forecast cycle: The Rapid Refresh. *Mon. Wea. Rev.*, **144**, 1669–1694, https://doi.org/10.1175/MWR-D-15-0242.1.

Gal-Chen, T., and R. C. Somerville, 1975: On the use of a coordinate transformation for the solution of the Navier-Stokes equations. *J. Comput. Phys.*, **17**, 209–228, https://doi.org/10.1016/0021-9991(75)90037-6.

James, E. P., and S. G. Benjamin, 2017: Observation system experiments with the hourly updating rapid refresh model using GSI hybrid ensemble-variational data assimilation. *Mon. Wea. Rev.*, **145**, 2897–2918, https://doi.org/10.1175/MWR-D-16-0398.1.

Kim, J.-H., R. D. Sharman, S. Benjamin, J. Brown, S.-H. Park, and J. Klemp, 2019: Improvement of mountain-wave turbulence forecasts in NOAA's Rapid Refresh (RAP) model with the hybrid vertical coordinate system. *Wea. Forecasting*, **34**, 773–780, https://doi.org/10.1175/WAF-D-18-0187.1.

Klemp, J. B., 2011: A terrain-following coordinate with smoothed coordinate surfaces. *Mon. Wea. Rev.*, **139**, 2163–2169, https://doi.org/10.1175/MWR-D-10-05046.1.

Kurihara, Y., 1968: Note on finite difference expressions for the hydrostatic relation and pressure gradient force. *Mon. Wea. Rev.*, **96**, 654–656, https://doi.org/10.1175/1520-0493(1968)096<0654:NOFDEF>2.0.CO;2.

Mahrer, Y., 1984: An improved numerical approximation of the horizontal gradients in a terrain-following coordinate system. *Mon. Wea. Rev.*, **112**, 918–922, https://doi.org/10.1175/1520-0493(1984)112<0918:AINAOT>2.0.CO;2.

Mesinger, F., and Z. Janjić, 1985: Problems and numerical methods of the incorporation of mountains in atmospheric models. *Lect. Appl. Math.*, **22**, 81–120.

Neale, R. B., and Coauthors, 2012: Description of the NCAR Community Atmosphere Model (CAM 5.0). NCAR Tech. Note NCAR/TN-486+STR, 274 pp., www.cesm.ucar.edu/models/cesm1.0/cam/docs/description/cam5_desc.pdf.

Park, S.-H., W. C. Skamarock, J. B. Klemp, L. D. Fowler, and M. G. Duda, 2013: Evaluation of global atmospheric solvers using extensions of the Jablonowski and Williamson baroclinic wave test case. *Mon. Wea. Rev.*, **141**, 3116–3129, https://doi.org/10.1175/MWR-D-12-00096.1.

——, J.-H. Kim, R. D. Sharman, and J. B. Klemp, 2016: Update of upper level turbulence forecast by reducing unphysical components of topography in the numerical weather prediction model. *Geophys. Res. Lett.*, **43**, 7718–7724, https://doi.org/10.1002/2016GL069446.

——, J. B. Klemp, and J.-H. Kim, 2019: Hybrid mass coordinate in WRF-ARW and its impact on upper-level turbulence forecasting. *Mon. Wea. Rev.*, **147**, 971–985, https://doi.org/10.1175/MWR-D-18-0334.1.

Peckham, S. E., T. G. Smirnova, S. G. Benjamin, J. M. Brown, and J. S. Kenyon, 2016: Implementation of a digital filter initialization in the WRF model and its application in the Rapid Refresh. *Mon. Wea. Rev.,* **144**, 99–106, https://doi.org/10.1175/MWR-D-15-0219.1.

Phillips, N. A., 1957: A coordinate system having some special advantages for numerical forecasting. *J. Meteor.*, **14**, 184–185, https://doi.org/10.1175/1520-0469(1957)014<0184:ACSHSS>2.0.CO;2.

Schär, C., D. Leuenberger, O. Fuhrer, D. Lüthi, and C. Girard, 2002: A new terrain-following vertical coordinate formulation for atmospheric prediction models. *Mon. Wea. Rev.*, **130**, 2459–2480, https://doi.org/10.1175/1520-0493(2002)130<2459:ANTFVC>2.0.CO;2.

Sharman, R., C. Tebaldi, G. Wiener, and J. Wolff, 2006: An integrated approach to mid- and upper-level turbulence forecasting. *Wea. Forecasting*, **21**, 268–287, https://doi.org/10.1175/WAF924.1.

Skamarock, W. C., and Coauthors, 2008: A description of the Advanced Research WRF version 3. NCAR Tech. Note NCAR/TN-475+STR, 113 pp., https://doi.org/10.5065/D68S4MVH.

——, and Coauthors, 2019: A description of the Advanced Research WRF version 4. NCAR Tech. Note NCAR/TN-556+STR, 145 pp., https://doi.org/10.5065/1dfh-6p97.

Smith, M. B., R. T. Pierce, J. A. Hamilton, K. L. Holub, B. Strong, and D. D. Turner, 2019: Development of GSD's Model Analysis Tool Suite (MATS). *35th Conf. on Environmental Information Processing Technologies*, Phoenix, AZ, Amer. Meteor. Soc., 12A.3, https://ams.confex.com/ams/2019Annual/webprogram/Paper353339.html.

Smith, T. L., S. G. Benjamin, J. M. Brown, S. Weygandt, T. Smirnova, and B. Schwartz, 2008: Convection forecasts from the hourly updated, 3-km High Resolution Rapid Refresh (HRRR) model. *24th Conf. on Severe Local Storms*, Savannah, GA, Amer. Meteor. Soc., 11.1, https://ams.confex.com/ams/24SLS/techprogram/paper_142055.htm.

Weatherhead, E. C., and Coauthors, 1998: Factors affecting the detection of trends: Statistical considerations and applications to environmental data. *J. Geophys. Res.*, **103**, 17 149–17 161, https://doi.org/10.1029/98JD00995.

Zängl, G., 2003: A generalized sigma-coordinate system for the MM5. *Mon. Wea. Rev.*, **131**, 2875–2884, https://doi.org/10.1175/1520-0493(2003)131<2875:AGSSFT>2.0.CO;2.